binding sites were completely saturated in SN-1 and SN-2 samples.
8. P. Sherline, C. Bodwin, D. M. Kipnis, *Anal. Biochem.* **62**, 400 (1974).
9. Tubulin was purified from rat brain [G. M. Fuller, B. R. Brinkley, J. M. Boughter, *Science* **187**, 948 (1975)] and iodinated with ^{125}I (New England Nuclear) [W. M. Hunter and F. C. Greenwood, *Nature (London)* **194**, 495 (1962); S. A. Berson and R. S. Yalow, in *Methods in Investigative and Diagnostic Endocrinology*, S. A. Berson and R. S. Yalow, Eds. (American Elsevier, New York, 1973), part 2A, p. 84].
10. S. Inoué, in *Primitive Motile Systems in Cell Biology*, R. D. Allen and N. Kamija, Eds. (Academic Press, New York, 1964), p. 549; O. Behnke and A. Forer, *J. Cell Sci.* **2**, 169 (1967).
11. W. J. Malaisse, F. Malaisse-Lagae, P. H. Wright, *Am. J. Physiol.* **213**, 843 (1967); N. J. Grey, S. Goldring, D. M. Kipnis, *J. Clin. Invest.* **49**, 881 (1970).
12. K. D. Buchanan, J. E. Vance, R. H. Williams, *Metabolism* **18**, 155 (1969).
13. C. J. Hedeskov and K. Capito, *Biochem. J.* **140**, 423 (1974).
14. H. Selawry, N. Voyles, R. Gutman, A. Wade, G. Fink, L. Recant, *Diabetes* **21**, 329 (1972).
15. S. Howell, I. C. Green, W. Montague, *Biochem. J.* **136**, 343 (1973).
16. G. M. Grodsky, H. Landahl, D. Curry, L. Bennett, in *Structure and Metabolism of the Pancreatic Islets*, S. Falkmer, B. Hellman, I. B. Taljedal, Eds. (Pergamon, Oxford, 1970), p. 409.
17. P. E. Lacy, *Nobel Symposium 13, Pathogenesis of Diabetes Mellitus*, E. Cerasi and R. Luft, Eds. (Almqvist & Wiksell, Uppsala, 1970), p. 108.
18. W. J. Malaisse, F. Malaisse-Lagae, M. M. Walker, P. E. Lacy, *Diabetes* **20**, 257 (1971).
19. H. Sando and G. M. Grodsky, *ibid.* **22**, 354 (1973).
20. D. G. Pipeleers, M. A. Pipeleers-Marichal, W. J. Malaisse, *Endocrinology* **93**, 1001 (1973).
21. This work was supported by PHS grant AMO 1921, by a research fellowship of the Belgian "National Fonds Wetenschappelijk Onderzoek" to D.G.P., and Harkness fellowship to D.G.P. We thank Mrs. N. Raymond-McGregor for valuable technical assistance and Dr. P. E. Lacy for discussion and criticism.

16 June 1975; revised 6 August 1975

Extracellular Potassium Accumulation and Inward-Going Potassium Rectification in Voltage Clamped Ventricular Muscle

Abstract. *Measurements of afterpotential, action potential duration, and output of a potassium-sensitive microelectrode indicate that the application of long clamp pulses (1 to 8 seconds) to frog ventricular muscle is accompanied by a change in the extracellular potassium concentration. The plot of the magnitude of the potassium accumulation against the clamped membrane potential yields an N-shaped relation similar to the "steady state" current-voltage relation. The accumulation studies confirm a strong inward-going (anomalous) potassium rectification.*

It is generally accepted that K efflux plays an important role in the repolarization of the cardiac action potential. Attempts to measure time-dependent changes in the radioactive K efflux during a single action potential have been made by using rapid perfusion. The results, however, indicated that diffusion across an unstirred extracellular space delays the efflux to the perfusing solution up to several seconds (*1*). The presence of a diffusion barrier may lead to poor time resolution of flux measurements, false low estimates of unidirectional transmembrane fluxes, and accumulation of K in the extracellular space.

In the experiments reported here, we have attempted to measure changes in the extracellular K concentration and relate them to the net membrane currents measured during a voltage clamp step. To estimate these changes, we have taken advantage of the specific effect of K on the resting potential (*2*) and on the duration of the action potential (*3*) of frog ventricular muscle. In some experiments the K activity was directly measured with a K-sensitive microelectrode (*4*) inserted into the preparation.

Strips of frog ventricular muscle (0.3 to 0.5 mm in diameter) were mounted in a single sucrose gap voltage clamp setup (*5*). Isometric tension, transmembrane potential, and membrane current were monitored simultaneously from the segment of muscle (length $\simeq$ 0.5 mm) bathed in Ringer solution (116 m*M* NaCl, 3 m*M* KCl, 2 m*M* $NaHCO_3$, and 0.2 m*M* $CaCl_2$). The other end of the muscle was depolarized with 120 m*M* KCl solutions. All experiments were performed at room temperature (20° to 24°C). In these experiments no corrections were made for "leakage current" across the sucrose gap or for potential drop across the series resistance. The preparation was considered to be satisfactory only if the current trace was smooth, without any indication of an inverted action potential, and the tension trace was free of transient contractile responses and well maintained during the clamp pulse.

Figure 1, A to D, shows voltage clamp steps to various potentials and the accompanying contractions and membrane currents superimposed on the normal action potential and contraction. The amplitude and time course of the afterpotential are monitored after releasing the clamp by opening the feedback loop. Five superimposed clamp steps are shown in each panel. In Fig. 1E the afterpotentials from A to D are plotted as functions of the clamp duration. In Fig. 1A, where the membrane is hyperpolarized from rest (from –85 to –106 mv), a hyperpolarizing afterpotential develops rapidly while the inward current decreases. In Fig. 1B the membrane is depolarized to –43 mv; the outward current is fairly constant, and the afterpotentials seem to approach a constant value. Clamp pulses of 2 seconds or less, which are accompanied by fairly con-

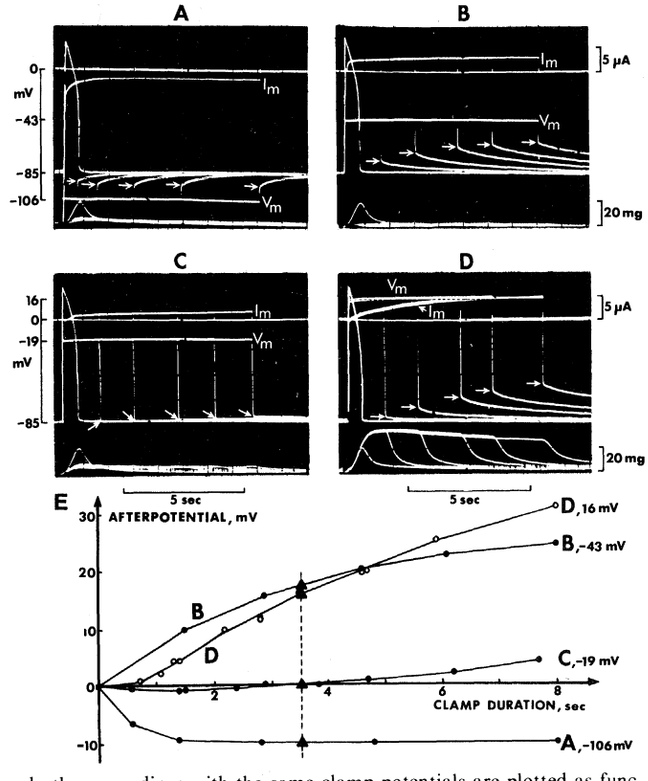

Fig. 1. Afterpotential as a function of clamp duration for four different clamp potentials: (A) –106 mv, (B) –43 mv, (C) –19 mv, and (D) +16 mv). In each panel five clamp pulses and the associated membrane currents and contractions are superimposed on a normal action potential and contraction. The continuous horizontal line near the top of each panel is the zero current trace. The current trace is labeled I_m and the membrane potential during the clamp is labeled V_m. The afterpotentials are measured shortly after release of the clamps as the difference between the resting potential and the potentials at the sharp bends indicated with arrows. Bottom traces are contraction recordings. (E) Afterpotentials from the recordings in (A) to (D) and other recordings with the same clamp potentials are plotted as functions of clamp duration. The dashed line indicating a clamp duration of 3.4 seconds intersects the curves in points marked with triangles and corresponding to values plotted in Fig. 2.

stant current traces, show a linearly increasing afterpotential. In Fig. 1C, where the membrane is depolarized to −19 mv, the current increases very slowly and there is little or no depolarizing afterpotential following the release of the clamp. In this region of membrane potential, where the "steady state" current-voltage relation has a minimum, the afterpotential often starts as a small hyperpolarizing potential, changing in time into a depolarizing afterpotential. In Fig. 1D the membrane potential is depolarized to +16 mv; the current is initially very small but then approaches a large outward value. The afterpotential develops with some delay, but then continues to increase even at the end of an 8-second clamp step tested in this experiment.

An estimate of whether the measured current is large enough to account for the observed afterpotential is made by comparing the membrane current (2.5 μa in Fig. 1B) with the rate of development of the afterpotential (7 mv/sec). In 1 second a current of 2.5 μa carries 2.5 μc or 2.5×10^{-11} equivalents across the membrane. In these preparations [length $\simeq$ 0.5 mm, diameter $\simeq$ 0.4 mm, and extracellular space $\simeq$ 25 percent (*6*)] the volume of the extracellular space is approximately 0.5 mm $\times$ (0.4 mm)^2 $\times$ 0.25 $\times$ (π/4) $\times$ 10^{-6} liter/mm^3 = 1.5×10^{-8} liter. If all the current was carried by K^+, the concentration of this ion in the extracellular space would increase as much as (2.5×10^{-11} mole)/(1.5×10^{-8} liter) = 1.67 m*M*. With this amount of K added to the normal concentration of K in the Ringer solution (3 m*M*), the membrane potential would change by 11 mv if the membrane followed the Nernst equation [58 mv $\times$ $\log_{10}$(3 + 1.67)/3 = 11 mv]. The agreement with the measured 7-mv afterpotential is fairly good when it is considered that the size of the preparation is roughly estimated, that the membrane current is overestimated because of leakage current, and that the resting potential only partially follows the K potential (*2*). It is also possible that the initial accumulation is limited to a fraction of the extracellular space ($\sim$ one-third) found inside the endothelial sheath surrounding individual muscle bundles (*7*). The half-time for the decay of the afterpotentials (1 to 3 seconds) is comparable to the half-time calculated for the diffusion equilibration of Ca through the narrow clefts of the endothelial sheath (2.3 seconds) or the half-time for the fast inotropic response to changes in the Ca concentration of the perfusing solution (3 to 10 seconds).

The afterpotentials following short clamp pulses seems to be related to the integral of the membrane current; however, with longer clamp pulses the afterpotentials develop more slowly. Much

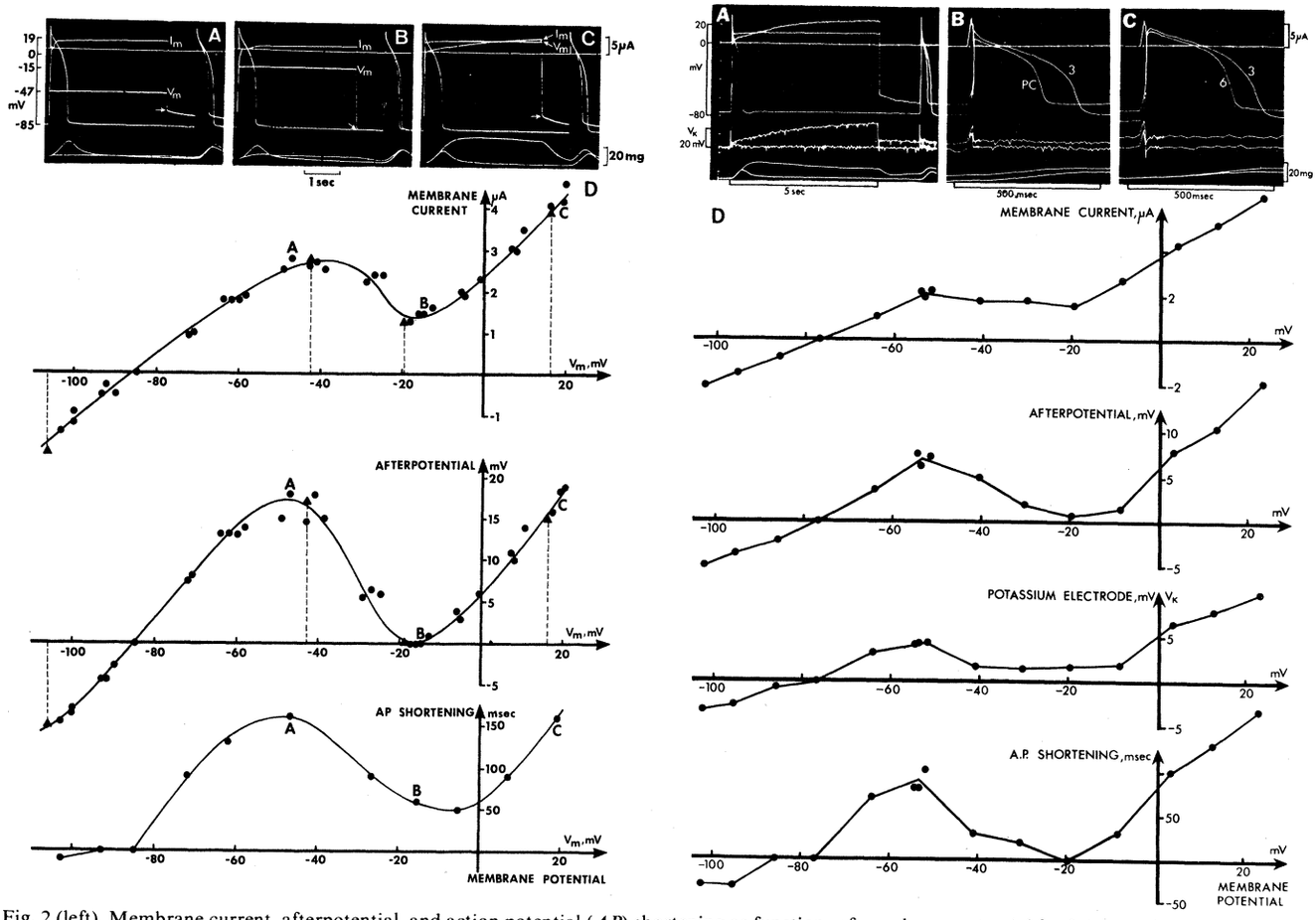

Fig. 2 (left). Membrane current, afterpotential, and action potential (*AP*) shortening as functions of membrane potential for 3.4-second clamp pulses. (A to C) A sweep with a clamp pulse followed 800 msec later by an action potential is superimposed on a sweep with two normal action potentials, 4.2 seconds apart. The membrane current is measured just before and the afterpotential just after release of the clamp. (D) Circles indicate results obtained with 3.4-second clamp pulses. The points measured from the recordings in (A), (B), and (C) are marked accordingly. Triangles in combination with dashed lines represent interpolated values from Fig. 1, which was obtained from the same preparation. Fig. 3 (right). Membrane current, afterpotential, output of a K electrode, and action potential (*AP*) duration as functions of membrane potential for 5-second clamp pulses. The graphs in (D) are based on recordings like those in (A) and (B). (A) A sweep with a clamp pulse followed by an action potential is superimposed on a sweep with two normal action potentials 6.6 seconds apart. The action potential following the clamp pulse (*PC*) and a normal action potential (3 m*M*) are shown with expanded time base in (B). From the top, the traces are: membrane potential and membrane current with a common baseline, the trace from the K-sensitive electrode, and the tension trace. A digital computer was used for sampling, replay, and analysis of the traces. The membrane current is measured at the end of the clamp. Afterpotential and the potential from the K-sensitive electrode are measured just before stimulation of the test action potential. (C) Action potentials and K electrode recordings before and after changing the K concentration of the perfusing solution from 3 m*M* to 6 m*M*.

larger extracellular K accumulation has also been observed in the giant axon of the squid (*8*). This may be due in part to larger K currents (of the order of milliamperes per square centimeter as compared to a few microamperes in heart muscle).

Figure 2 shows the results obtained when clamp pulses of fixed duration, 3.4 seconds, were applied to study the afterpotential as a function of the clamped membrane potential in greater detail. The duration of a test action potential generated 800 msec after release of the clamp is compared to that of a normal action potential. The membrane current at the end of the clamp pulse, the afterpotential, and the action potential shortening are plotted against the clamped membrane potential. Both afterpotential and action potential shortening yield N-shaped relations similar to the current-voltage relation. Such results indicate that the K efflux has a minimum in the same voltage region as the membrane current.

In the experiment of Fig. 3, a K-sensitive microelectrode directly monitoring the local extracellular K activity was inserted into another preparation. The electrodes were prepared by filling the glass micropipette with a liquid ion exchange resin (*4*, *9*). The tip diameter was ~ 1 μm and the electrochemical response time ranged between 15 and 25 msec (*10*). With the electrode placed in the muscle, the measured potential is the sum of the potential caused by changes in the K activity and the electrical potential in the extracellular space. During the application of a voltage clamp step the flow of current through the series resistance adds to the electrical signal resulting from K accumulation. However, after the release of the clamp step, when there is no applied current, the K electrode trace mainly represents the K activity in the extracellular space and exhibits a slowly decaying tail similar to the time course of the afterpotential (Fig. 3A). In Fig. 3D the current at the end of the clamp, the afterpotential, the signal from the K-sensitive microelectrode, and the action potential shortening are all plotted against the clamped membrane potential. In this experiment the afterpotential and the response from the K electrode were measured just before the test action potential was generated in order to obtain a more accurate estimate of the extracellular K^+ concentration at the time of the test action potential generation. Note that the three parameters used to estimate the extracellular K concentration all yield N-shaped relations with a minimum around –20 mv, similar to the steady state current-voltage relation. These results provide strong evidence for inward-going (anomalous) rectification of the K current. Although the negative slope of the steady state current-voltage relation between –40 and –20 mv could be explained by the turn-on of an inward current component (Na or Ca), the decreasing accumulation in this region can only be explained by the turn-off of the K current.

Although afterpotential, K electrode, and action potential shortening give basically the same voltage dependence for the K accumulation, there are minor systematic differences. The action potential shortening after clamps to or above plateau level is often greater than that observed when the same afterpotentials are obtained after clamps to lower voltages. This effect is most prominent when the action potential is stimulated shortly after the end of the clamp. The action potential prolongation following hyperpolarizing clamps is often very small, although there is a considerable hyperpolarizing afterpotential. In Fig. 3A the K electrode potential has a smaller shift and a slower initial decay than the afterpotential. This suggests that the K electrode either is less sensitive to K than the myocardial membrane or is exposed to a smaller change in the K concentration. The first possibility is tested by the experiment in Fig. 3C, where the K concentration is changed from 3 to 6 m*M*. The very similar depolarizations measured with the K electrode (11 mv) and the intracellular microelectrode (12 mv) do not, however, indicate significant differences in K selectivity. The afterpotential probably reflects the average K concentration in the immediate vicinity of the membrane, while the K electrode measures a lower and more localized concentration change in one of the larger compartments of the extracellular space. The considerable outward current recorded at the minimum of the current-voltage relation in combination with little or no depolarizing afterpotential suggests that the steady state current includes other components than the K current (such as the Cl current, the transgap leakage current, and the current associated with an electrogenic Na-K pump).

These experiments show that extracellular K accumulation does occur in frog ventricular muscle during long clamp pulses. The time and voltage dependence of the accumulation indicates that it is closely related to the membrane current and thus can be used as an indicator for K efflux. In this capacity the accumulation verifies inward-going K rectification.

LARS CLEEMANN, MARTIN MORAD
Department of Physiology, University of Pennsylvania School of Medicine, Philadelphia 19174

References and Notes

1. J. F. Lamb and J. A. S. McGuigan, *J. Physiol. (Lond.)* **195**, 283 (1968).
2. A. J. Brady and J. W. Woodbury, *ibid.* **154**, 385 (1960).
3. S. Weidmann, *ibid.* **132**, 157 (1956).
4. J. Walker, *Anal. Chem.* **43**, 89A (1971).
5. M. Morad and R. K. Orkand, *J. Physiol. (Lond.)* **219**, 167 (1971).
6. M. J. Keenan and R. Niedergerke, *ibid.* **188**, 235 (1967).
7. S. G. Page and R. Neidergerke, *J. Cell Sci.* **11**, 179 (1972).
8. B. Frankenhaeuser and A. L. Hodgkin, *J. Physiol. (Lond.)* **131**, 341 (1956), W. J. Adelman, Jr., Y. Palti, J. P. Senft, *J. Membr. Biol.* **13**, 387 (1973).
9. Corning No. 477317.
10. R. P. Kline and M. Morad, in preparation.
11. We thank R. P. Kline for providing us with K electrodes. Supported by PHS grant 16152.

20 June 1975; revised 22 September 1975

Serengeti Migratory Wildebeest: Facilitation of Energy Flow by Grazing

Abstract. *Dense concentrations of migratory wildebeest leaving the Serengeti Plains in late May 1974 reduced green plant biomass by almost 400 grams per square meter, 85 percent of the initial standing crop. However, this grazing prevented senescence and stimulated net primary productivity of the grasslands. Thomson's gazelles leaving the plains a month later were significantly associated with areas previously grazed by wildebeest, and this association was still evident at the end of the dry season, 6 months later.*

The Serengeti-Mara ecosystem is defined by the movement of the region's large herds of migratory grazers (*1*), and consists of core areas in Tanzania's Serengeti National Park and Kenya's Maasai-Mara Game Reserve, together with adjacent areas. This region contains "the greatest and most spectacular concentration of game animals found anywhere in the world" (*2*). The most recent population estimates suggest a 1974 population size of more than 1 million wildebeest (*Connochaetes taurinus albojubatus* Thomas) (*3*), 600,000 Thomson's gazelle (*Gazella thomsonii*) (*4*), 200,000 zebra (*Equus burchelli*) (*5*), and 65,000 buffalo (*Syncerus caffer* Spearman) (*6*), as well as undefined numbers of more than 20 other species of grazing animals. There is, however, very little information on the dynamics of the grasslands supporting this huge herbivore biomass. The information reported here on productivity of the grasslands along the western border of the Serengeti Plains indicates that the migratory wildebeest convert a senescent grassland into a highly